RM L57E15

NACA

RESEARCH MEMORANDUM

EXPERIMENTAL INVESTIGATION OF WING-AILERON FLUTTER

CHARACTERISTICS OF A 1/4-SCALE DYNAMIC

MODEL OF THE X-1E AIRPLANE

By Frederick W. Gibson, William B. Igoe,
and P. R. Maloney

Langley Aeronautical Laboratory
Langley Field, Va.

NATIONAL ADVISORY COMMITTEE
FOR AERONAUTICS

WASHINGTON
July 10, 1957
Declassified January 12, 1961

NATIONAL ADVISORY COMMITTEE FOR AERONAUTICS

RESEARCH MEMORANDUM

EXPERIMENTAL INVESTIGATION OF WING-AILERON FLUTTER

CHARACTERISTICS OF A 1/4-SCALE DYNAMIC

MODEL OF THE X-1E AIRPLANE

By Frederick W. Gibson, William B. Igoe,
and P. R. Maloney

SUMMARY

Tests to determine some of the flutter characteristics of a 1/4-scale dynamic model of the X-1E airplane wing and aileron were made in the Langley 16-foot transonic tunnel. The wing was tested as part of a complete model of the airplane over a Mach number range of 0.4 to 1.05. Fuselage angles of attack were varied from -14° to 15° at low Mach numbers and from -5° to 4° at higher Mach numbers. Static loading and vibration tests were also performed in still air.

No stall flutter or classical flutter was encountered; however, the test results indicate that unstable aeroydnamic damping is present on the ailerons at transonic speeds. The aileron flutter response to this unstable aerodynamic damping is influenced by the free play in the aileron control system - increasing free play expands the flutter region. It was shown that this flutter response could be eliminated by adding viscous damping directly to the ailerons.

INTRODUCTION

The low-altitude flight program for the X-1E airplane requires that the airplane be flown to supersonic speeds at a minimum altitude of 30,000 feet. In addition, an air launch of the X-1E at 30,000 feet at a Mach number of 0.6 is required. Some limited analytical and experimental investigations indicated that the aileron torsion flutter, aileron single-degree-of-freedom flutter or buzz, and stall-flutter characteristics of the wing were marginal. As a consequence of these preliminary indications of small flutter margins, it was deemed desirable to reproduce in a model the aileron control system of the aircraft, as well as other wing properties, in as great detail as possible, in order to attain

a realistic approximation of the dynamic behavior of the full-scale wing, aileron control system, and aileron dampers. Therefore, a 1/4-scale dynamic model of the X-1E wing was constructed to meet these requirements and tested as part of the complete-model configuration in the Langley 16-foot transonic tunnel.

The purpose of this paper is to present the results of the ground vibration and wind-tunnel tests of this model.

SYMBOLS

D   damping, lb-sec/ft

EI   wing bending rigidity, lb-in.^{2}

GJ   wing torsional rigidity, lb-in.^{2}

M   Mach number

ρ mass density, slugs/cu ft

ω frequency of oscillation, radians/sec

λ geometric scale factor, l_M/l_F

l general dimension of length

m   mass per unit length, lb-sec^2/sq in.

I   mass polar moment of inertia per unit length, lb-sec^2

g   structural damping coefficient

Subscripts:

M   model

F   full scale

DESIGN AND CONSTRUCTION DETAILS

Selection of Scale Factors

It was desired to design the model wing to be a true-speed dynamic replica of the X-1E airplane wing. The quantities available for scaling were linear dimensions, mass, moments of inertia, frequencies, and stiffnesses of the full-scale wing. While structural damping was not scaled directly, it was hoped that a fairly complete physical representation of the airplane wing structure would give a close representation of the full-scale airplane damping. In order to reduce scale effects, the model was made as large as possible for the Langley 16-foot transonic tunnel. This resulted in a geometric scale factor λ of 1/4.

In designing the model, it was desirable to simulate the proposed operational altitude conditions of the full-scale airplane. Since a tentative flight plan for the X-1E airplane called for it to be launched at an altitude of 30,000 feet and flown through the transonic-speed range at that altitude, this was considered to be the desired full-scale altitude to be simulated. The 16-foot transonic tunnel has a variation of test-section air density and a corresponding variation of density altitude with Mach number, as shown in figure 1 for atmospheric stagnation conditions. It was desired to satisfy the mass-density-ratio conditions for the model at $M = 1.0$ where the equivalent density altitude of the wind tunnel corresponded to approximately 15,000 feet. At an altitude of 15,000 feet the density is approximately 68 percent greater than the density at 30,000 feet; therefore, to satisfy the mass-density-ratio conditions, the model should have been 68 percent heavier than the full-scale airplane. In order to achieve the same aeroelastic effects under the airloads, the model should have been 68 percent stiffer also. However, preliminary studies of the model design showed that the maximum practical increase possible in model stiffness (for the material and type of construction selected) was about 50 percent; therefore, a factor of 1.5 was accepted as a design figure for the increase in model density and stiffness. The density altitude for which the full-scale airplane was simulated by the model in the wind tunnel for the density factor of 1.5 is also shown in figure 1. The following table lists the scaled quantities in terms of the geometric scale factor λ and includes the 1.5 stiffness and density factor:

Quantity	Scale factor
Mass per unit length, m_M/m_F	$1.5 \times \lambda^2 = 1.5/16$
Mass moment of inertia per unit length, I_M/I_F . . .	$1.5 \times \lambda^4 = 1.5/256$
Frequency, ω_M/ω_F	$1/\lambda = 4$
Bending stiffness, EI_M/EI_F	$1.5 \times \lambda^4 = 1.5/256$
Torsion stiffenss, $(GJ)_M/(GJ)_F$	$1.5 \times \lambda^4 = 1.5/256$

Full-Scale Design and Construction

The airplane wing has an NACA 64A004 (modified) airfoil section, 2° incidence with respect to the fuselage with zero twist, a taper ratio of 0.5, an aspect ratio of 4, and zero sweep of the 40-percent-chord line. For structural reasons, the airfoil section is modified so that it has a straight taper from the 70 percent chord line to the trailing edge, which has a thickness of 0.36 percent of chord. The aileron is 30 percent of the wing chord and extends spanwise from 68 percent to 98 percent of the wing semispan.

The construction characteristics of the full-scale wing are illustrated in figure 2(a). The leading edge is solid, and spar and web members are solid and nearly rectangular sections, the web members being staggered as shown. One-eighth-inch stainless-steel doublers are sandwiched between the upper and lower skins and the spars and extend out from the center line over approximately 42 percent of the semispan. The skin is a continuous sheet having a thickness of 0.608 percent of the chord outboard of the 20-percent-semispan station and a constant thickness of 0.5 inch inboard of that station and is designed to provide all the strength in the wing. The leading edge, skin, webs, and spars are 7075-T aluminum alloy. The right and left semispans of the airplane wing are spliced together at the center line. The wings are fixed to the fuselage with four-point suspension as shown in figure 2(b). The aileron has chordwise tapered skins on Z-section ribs rearward of the hinge line. The leading edge has a lead cap along the span. The aileron is essentially steel forward of the hinge line with the exception of the lead cap and is statically balanced about the hinge line.

The aileron control system is wholly mechanical, comprised of a system of yokes, bell cranks, idlers, and push-pull rods. Figure 2(c) shows the general configuration of the full-scale aileron control system.

Model Wing Design and Construction

In order to satisfy the requirements imposed on the model by the tunnel conditions, the model was designed and constructed in the following manner: The spars and web members were machined as an integral unit from a sheet of aluminum, and the skin thickness was increased from 0.608 to 1.0 percent of the chord. In order to maintain the 4-percent-thickness ratio, the material could only be added inside the wing near the neutral axis where the effect on the moment of inertia is reduced. As a result, the bending and torsional stiffnesses were increased by approximately 50 percent. As previously noted, this increase was finally accepted as the maximum obtainable inasmuch as it was necessary to retain ribs, spars, and space for the installation of the aileron control system.

It would also have been desirable to place the doublers inside the wing as on the full-scale airplane, but, because of the thickened skin, the doublers would have been so close to the neutral axis that their effect would have been very small. Therefore, to minimize the amount of material that would be needed for the doublers to bring the wing up to the desired stiffness, the core in the area of the doublers was left solid and the remaining required stiffness added by bonding and riveting the appropriate thickness of doublers on the outside of the wing. This modification changed the maximum thickness ratio from 4 percent to about 4.5 percent in the area of the doublers. Figure 3(a) illustrates the construction details of the model wing.

The right and left semispans of the model wing were made integral to avoid making a splice. The stiffness of the full-scale airplane splice was simulated. The wings were fixed to the fuselage with a four-point suspension system the same as that for the airplane as shown in figure 2(b). Figure 3(b) is a sketch of the complete model mounted on the sting.

The aileron system of the model, like that of the airplane is wholly mechanical and contains bearings, idlers, bell cranks, and push-pull rods which were scaled as closely in size as the available bearing sizes would permit. The model aileron system is shown in figure 3(c).

Instrumentation of the Model

The model wing was instrumented to obtain instantaneous wing bending and torsion strains and the aileron was instrumented to obtain rotational angles about its hinge line. Three bending and three torsion strain gages were located near the wing-fuselage juncture of each semispan as shown in figure 4. Three position indicators, one flexible-beam type and two inductance type, located as shown in figure 4, were installed on the right aileron. A single flexible-beam-type indicator was attached to the left wing aileron.

The flexible-beam-type indicator consisted of a small flexible beam on which was bonded a strain gage. One end of this beam was fixed to the wing structure, and the other end was connected to the bell crank of the aileron control system so that the motion of the control system caused bending of the beam. This indicator was useful in obtaining records of the antisymmetric motion of the ailerons at low frequencies.

The electrical inductance-type indicator consisted of two coils and a metal vane in the field of the coils. Rotation of the vane or coils altered the output signal of the circuit. At the inboard end of the aileron, the coils were fixed to the wing and the vane moved with the aileron, while at the outboard end of the aileron the vane was fixed

and the coil moved. The frequency response of this type of indicator
was flat to over 500 cps.

                                Ground Tests

     Initial ground vibration and static loading tests of the 1/4-scale
model were made to determine the natural frequencies and the stiffness
and nodal characteristics of the wing, aileron, and aileron control
system and to calibrate the strain-gage and position-indicator systems.
The model wing mounted for ground testing is shown in figure 5. In the
ground tests of the model the support conditions of the ground tests on
the full-scale airplane were simulated as closely as was possible. For
the symmetric first bending mode and symmetric and asymmetric torsion
modes the section of the full-scale fuselage containing the wing was
mounted by bolting a rigid steel plate to each end of the fuselage sec-
tion and securing these plates to the concrete hangar apron by means of
a steel structure. For the model this condition was simulated by securing
the fuselage structure to a steel bed plate. For the asymmetric first
bending mode the full-scale airplane was supported on its landing gear
with 50 percent of normal air pressure in the tires. In order to simu-
late this condition, the 1/4-scale model was mounted on a dummy sting
which allowed translational motion.

     An optical system was used to measure deflections of the wing and
aileron under static loads and, with the aid of a shaker, to make
frequency-response surveys of the wing and ailerons.

     Two types of shakers were used to obtain frequency-response curves
and to make studies of the mode characteristics. Electromagnetic shakers
were used to study wing vibration characteristics. Two of these shakers
were fastened to the wing symmetrically with respect to the fuselage
center line at points close to the wing-fuselage juncture on the leading
edge. (See fig. 5.) Thus, with the shakers in phase or 180° out of
phase, the wings could be excited symmetrically or asymmetrically.
Because the electromagnetic shakers added considerable mass to the
ailerons, they could not be used to obtain the aileron frequencies.
Therefore, a pneumatic shaker was developed which employed pulsed air-
streams directed alternately against the upper and lower surfaces of
the aileron. This air shaker was used very successfully in obtaining
frequency-response surveys of both the model and full-scale ailerons.

     Model wing properties.- The degree of duplication of the physical
properties of the full-scale wing that was attained in the 1/4-scale
model is shown in figures 6 to 8 and in tables I and II. Table I com-
pares the full-scale and 1/4-scale nodal patterns and resonant frequen-
cies of the symmetric and asymmetric first bending and first torsion
modes where close similarity is shown. Figure 6 compares the spanwise

weight distributions which were determined by computations based on the
wing designs. The simulation here is only fair. Figure 7 compares the
torsional stiffness distributions where the similarity is fairly good
although the stiffness at the outboard half of the semispan of the model
is somewhat low. Figure 8 presents the measured values of EI of the
1/4-scale wing right and left semispans and the scaled computed values
of the full-scale wing. In this case the similarity is very good.

Model aileron properties.- The aileron system was nonlinear, the
nonlinearity being caused by the free play in the various linkages of
the control system.

The aileron stiffnesses, as presented in table II, were obtained
with the system locked at the center line of the fuselage, and the
angular motions referred to are aileron rotations about the hinge line.
Model stiffness at the bell crank (see fig. 3(b)) is 88 percent of the
design value. However, two values of stiffness were measured at the
root of the full-scale aileron at different times. The larger value was
found after the aileron system had been reworked to eliminate much of
the existing free play. The source of the discrepancy could not be
ascertained, but, because of the similarity in the scaled frequency of
the full-scale and the frequency of the 1/4-scale ailerons, it was
thought that the lower value of stiffness of the full-scale aileron at
the root was the more reliable.

The static and dynamic characteristics of the model ailerons were
found to vary with the amount of free play in the aileron control system
and with the amount of excitation force applied to the system. The free
play depended upon the tightness of fit of the pinned joints in the sys-
tem. The excitation force was regulated by the air pressure in the
pneumatic shaker. The characteristics of the aileron system are illus-
trated in figure 9.

Figure 9(a) shows the relationship between moment about the hinge
line and aileron deflection. The variation is linear except for a step
in the deflection which indicates the amount of free play in the system.
This characteristic of the model aileron is very similar to that which
was found on the full-scale aileron.

Figure 9(b) shows the variation of amplitude with frequency and
the effect of the magnitude of excitation force applied to the ailerons
on the resonant frequency and amplitude. Not only the amplitude but
also the resonant frequency increases with increased excitation force.

Figure 9(c) illustrates the effect of excitation force on the reso-
nant frequency for various degrees of free play in the system. Again
it is shown that increased excitation force causes increased resonant
frequency. It may also be seen that the resonant frequency is decreased
as the free play is increased.

In figure 9(d), frequency-response curves for several different values of excitation force are shown for both the model and the full-scale ailerons. This serves as an indication of the similarity of the combined effects of damping, stiffness, and inertia of the two systems.

The bump in the frequency-response curves below the resonant frequency of both the full-scale and 1/4-scale ailerons was caused by some excitation of a wing mode.

The effects of free play and amplitude of oscillation on the resonant frequency of the aileron system, as found in this investigation, are in agreement with the results of an analytical and experimental investigation reported in reference 1.

Aileron Dampers

The damping required to overcome the maximum unstable aerodynamic damping on the full-scale aileron was estimated from the data of reference 2. Aileron dampers were then designed for the model scaled from the full-scale dampers on the basis of $D_M = 1.5 D_F \lambda^2$ where D represents damping in pound-seconds per foot and M and F refer to the model and full-scale dampers, respectively. This relation was derived from the single-degree-of-freedom equation of motion for the aileron. The dampers were piston-type with a clearance between piston and cylinder. The supply of oil in the damper was maintained by pressure during operation. A cutaway sketch of the damper is shown in figure 10.

The dampers were first installed inside the wing with one end fixed to the wing and the other end connected to the bell crank as shown in figure 11(a). After numerous tests on the ground and in the wind tunnel it was apparent that the dampers located in this position were ineffective in eliminating the flutter condition. Repeated ground tests showed that with the same forcing function, the amplitude of oscillation was increased when the dampers were installed in this position. It was found that the dynamics of the system (including the free play) would not allow sufficient motion of the dampers in the ranges of amplitude of the ailerons which were of interest. Therefore, the dampers were mounted outside the wing with one end fixed to the wing and the other end connected directly to the aileron horn as shown in figure 11(b). Repeated ground tests with dampers in this position showed a decrease in the amplitude of oscillation. It was found that the static pressure of the fluid in the dampers had no apparent effect on the frequency response of the system.

Structural Damping of the Ailerons

The determination of the structural damping of the aileron system presented difficulty because of the nonlinearity caused by the free play in the system. Measurements were made of the structural damping by various methods both including and excluding the free play. The damping coefficient g was found to be of the order of 0.1 for an aileron rotational amplitude of about 0.6^O.

WIND-TUNNEL TESTS AND RESULTS

For the wind-tunnel tests, the 1/4-scale model of the X-1E airplane wing was assembled to an essentially rigid scale model of the X-1E fuselage and empennage. The model was sting mounted in the 16-foot transonic tunnel as shown in figure 12 and tested throughout the ranges of angles of attack and Mach numbers shown in figure 13 to study the stall flutter, classical flutter, and aileron flutter characteristics of the wing-aileron system. During the wind-tunnel tests, the aileron control column (see fig. 3(b)) was centered by a weak spring so that the ailerons were centered for zero load conditions. A pulsing device was used to give the ailerons an asymmetric deflection pulse of approximately 1^O under wind-off conditions. The pulsing device was effective at low tunnel airspeeds, but at higher tunnel airspeeds, where wind-tunnel turbulence contributed a fairly large exciting force to the ailerons, the aileron pulser was relatively ineffective.

No classical flutter or stall flutter was encountered throughout the range of the tests; however, an instability was experienced at transonic Mach numbers which involved considerable aileron motion and some wing torsional motion. Unfortunately, when aileron and wing motion occurred simultaneously, there was no way of determining definitely whether the phenomenon was aileron-torsion flutter or aileron buzz; however, it was the concerted opinion of the investigators that it was aileron buzz and therefore is referred to as such in the remainder of this paper.

Time-history records of the signal outputs of the strain gages and position indicators were made on an oscillograph. A typical example of an oscillograph record taken during the occurrence of aileron buzz is shown in figure 14.

The results of the wind-tunnel tests showing the effects of free play, angle of attack, aileron tabs, and aileron viscous dampers on aileron buzz were as follows:

Effect of free play.- The effect of free play in the aileron con-
trol system is illustrated in figure 15 where the flutter region is con-
tained within the boundaries shown. In this figure it may be seen that
the flutter boundary expands as the free play increases.

Effect of angle of attack.- Changing the angle of attack from the
condition of zero lift, which had the effect of placing a preload on
the aileron, eliminated the flutter condition - the amount of angle of
attack required depending on the amount of free play existing in the
aileron system. (See fig. 15.)

Effect of aileron viscous dampers.- Aileron viscous dampers were
tested with the dampers connected to the aileron bell crank as shown in
figure 11(a). The flutter region and the characteristics of the flutter
with the dampers in this position were substantially the same as without
dampers. The dampers were then moved to the position outside the wing
as shown in figure 11(b), that is, mounted directly between the aileron
horn and the wing structure. The flutter region was again explored and
it was found that, with the dampers mounted directly to the aileron,
the flutter condition was completely eliminated within the test limits.

As previously discussed, the reason for the ineffectiveness of the
dampers in limiting aileron flutter when connected to the bell crank
was the free play and structural compliance existing between the aileron
and the damper. These were reduced considerably when the dampers were
connected directly to the aileron horn.

Effect of aileron tabs.- In the course of the wind-tunnel tests,
aileron tabs (see fig. 2(b)) were tested to investigate the effect of
a preload on the ailerons on the flutter characteristics of the ailerons.
These tabs were 28.5 percent of the aileron span and extended rearward
9/16 inch from the aileron trailing edge. They were tested both at 0°
setting and -5°, that is, trailing edge down. At 0° setting the tabs
caused the aileron flutter boundary to be expanded slightly while at
-5° setting the flutter boundary was moved to slightly lower angles of
attack.

CONCLUDING REMARKS

An investigation has been made of the flutter characteristics of a
dynamically scaled model of the X-1E airplane wing. The dynamic prop-
erties of the full-scale X-1E airplane wing and aileron were well dupli-
cated in the 1/4-scale model. No stall flutter or classical flutter was
encountered. The critical Mach number and angle-of-attack ranges for
the X-1E model with respect to aileron flutter or buzz appear to be from
about 0.9 to 0.98 and from 1° to -4°, respectively. The effect of free

play in the aileron control system on the physical properties of the system was an important factor influencing aileron flutter. Aileron viscous dampers, when mounted to the aileron bell crank, with free play existing between the dampers and the aileron, proved to be ineffective in limiting aileron flutter. When the same viscous dampers were mounted directly between the aileron and the wing structure with little or no free play existing, aileron flutter or buzz was completely eliminated.
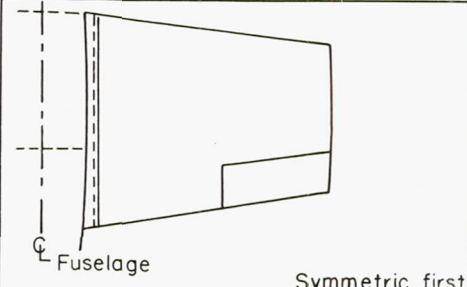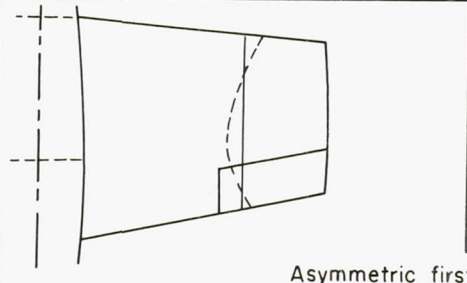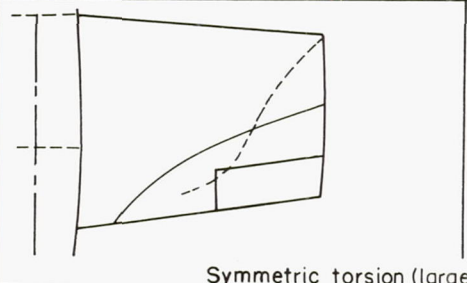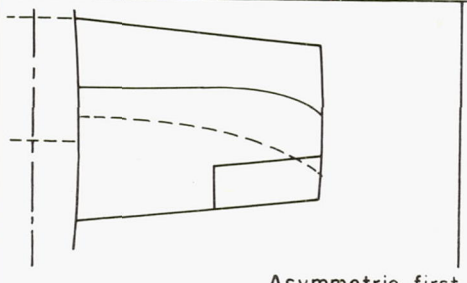
Langley Aeronautical Laboratory,
    National Advisory Committee for Aeronautics,
        Langley Field, Va., April 23, 1957.

<div align="center">REFERENCES</div>

1. Woolston, Donald S., Runyan, Harry L., and Andrews, Robert E.: An
    Investigation of Effects of Certain Types of Structural Nonline-
    arities on Wing and Control Surface Flutter. Jour. Aero. Sci.,
    vol. 24, no. 1, Jan. 1957, pp. 57-63.

2. Thompson, Robert F., and Moseley, William C., Jr.: Oscillating Hinge
    Moments and Flutter Characteristics of a Flap-Type Control Surface
    on a 4-Percent-Thick Unswept Wing With Low Aspect Ratio at Transonic
    Speeds. NACA RM L55K17, 1956.

TABLE I

WING MODE CHARACTERISTICS OF FULL-SCALE AND

1/4-SCALE X-1E AIRPLANE

Node lines	Full-scale 1/4-scale ⸻	Full-scale freq. × 1/λ , cps	1/4-scale frequency
Symmetric first bending		32.4	36.5
Asymmetric first bending		✶ 62	✶ 76 - 79
Symmetric torsion (large aileron response)		142	136.5
Asymmetric first torsion		114	123 - 125

✶ Full-scale airplane was mounted on landing gear with tires half inflated. 1/4-scale model was mounted on a dummy sting which allowed translational motion.

TABLE II

COMPARISON OF STIFFNESS CHARACTERISTICS OF 1/4-SCALE AND

FULL-SCALE X-1E WING AND AILERON

Parameter	Full-scale scaled values × 1.5	1/4-scale model values	Percent of design acquired in 1/4-scale model
Wing			
Torsional stiffness at wing tip, in-lb/radian	53,800	52,600	97.8
Bending stiffness at wing tip, lb/in.	326	308	94.5
Aileron			
Stiffness at root with control column locked, in-lb/deg	[a]25.5	21.3	[a]83.5
	[a]54.2		[a]39.3
Stiffness at bell crank with control column locked, in-lb/deg	160	141	88.1

[a]These values were found at different times. Reason for discrepancy could not be determined.
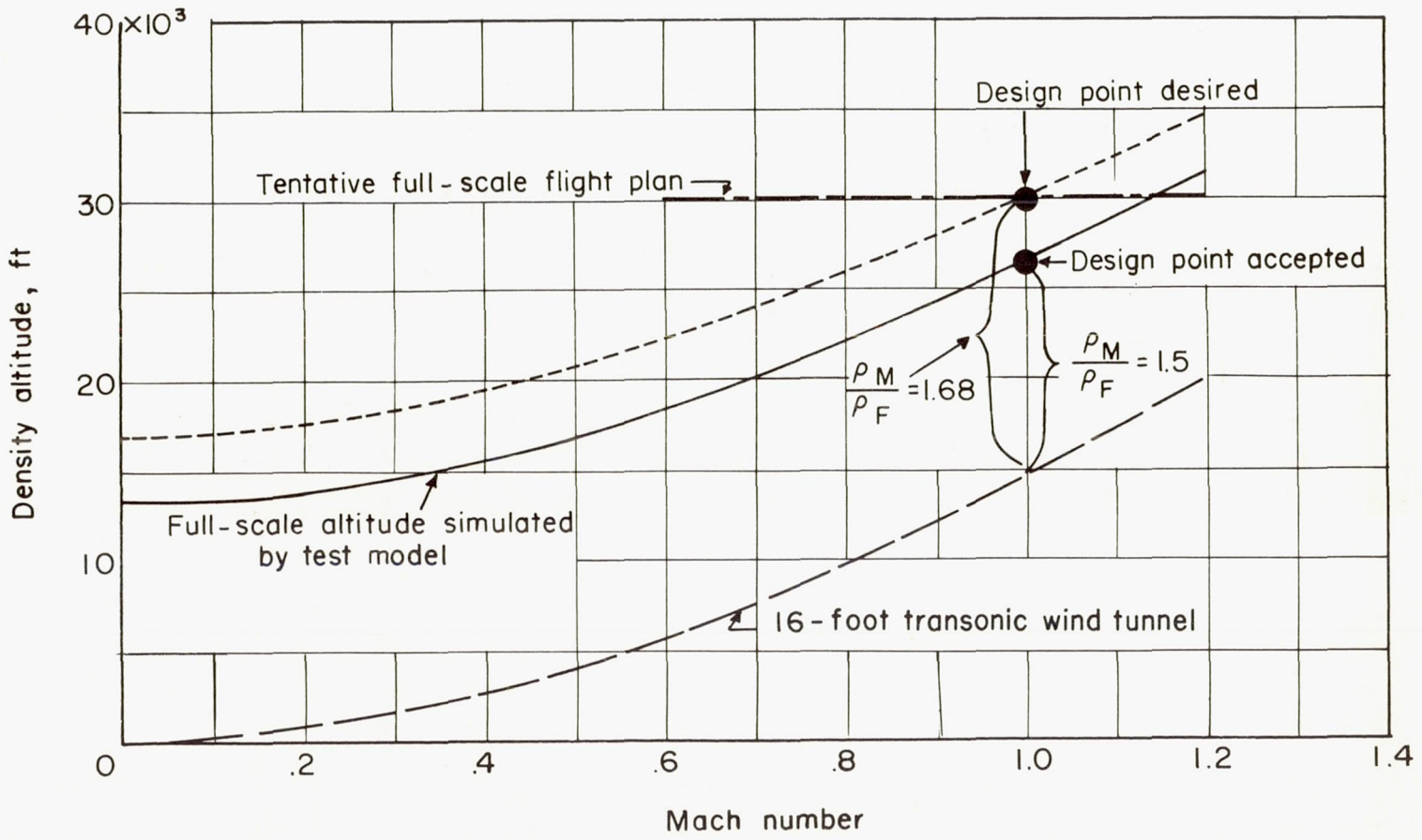
Figure 1.- Density-altitude simulation for model of X-1E airplane.

Doubler

Solid leading edge

Doublers

Solid tip

Aileron

Flap

A

A

CL
Fuselage
0   20   40   60   80   100   120   140

Wing station, in.
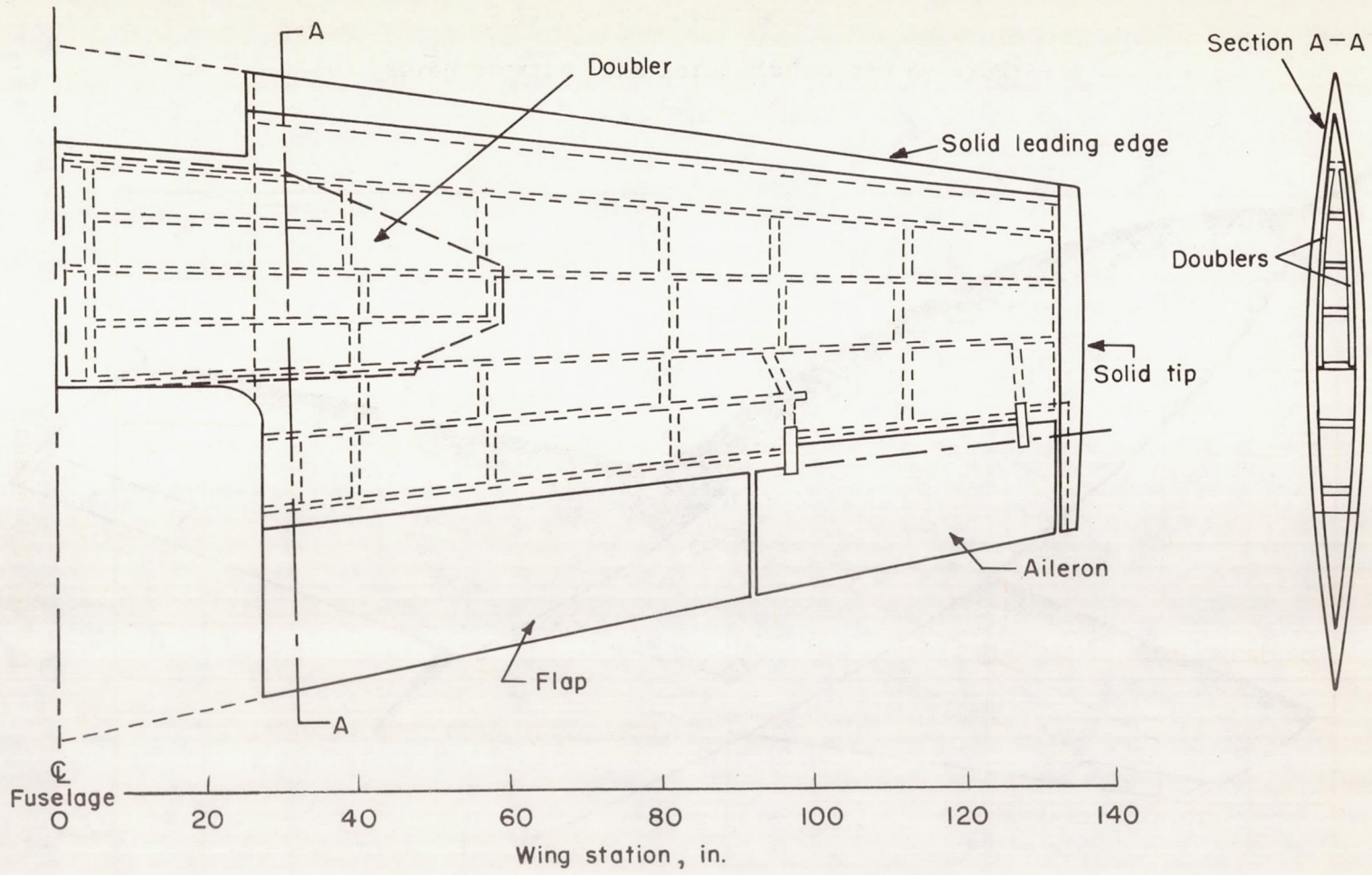
(a) Wing construction.

Figure 2.- Details of full-scale X-1E wing.
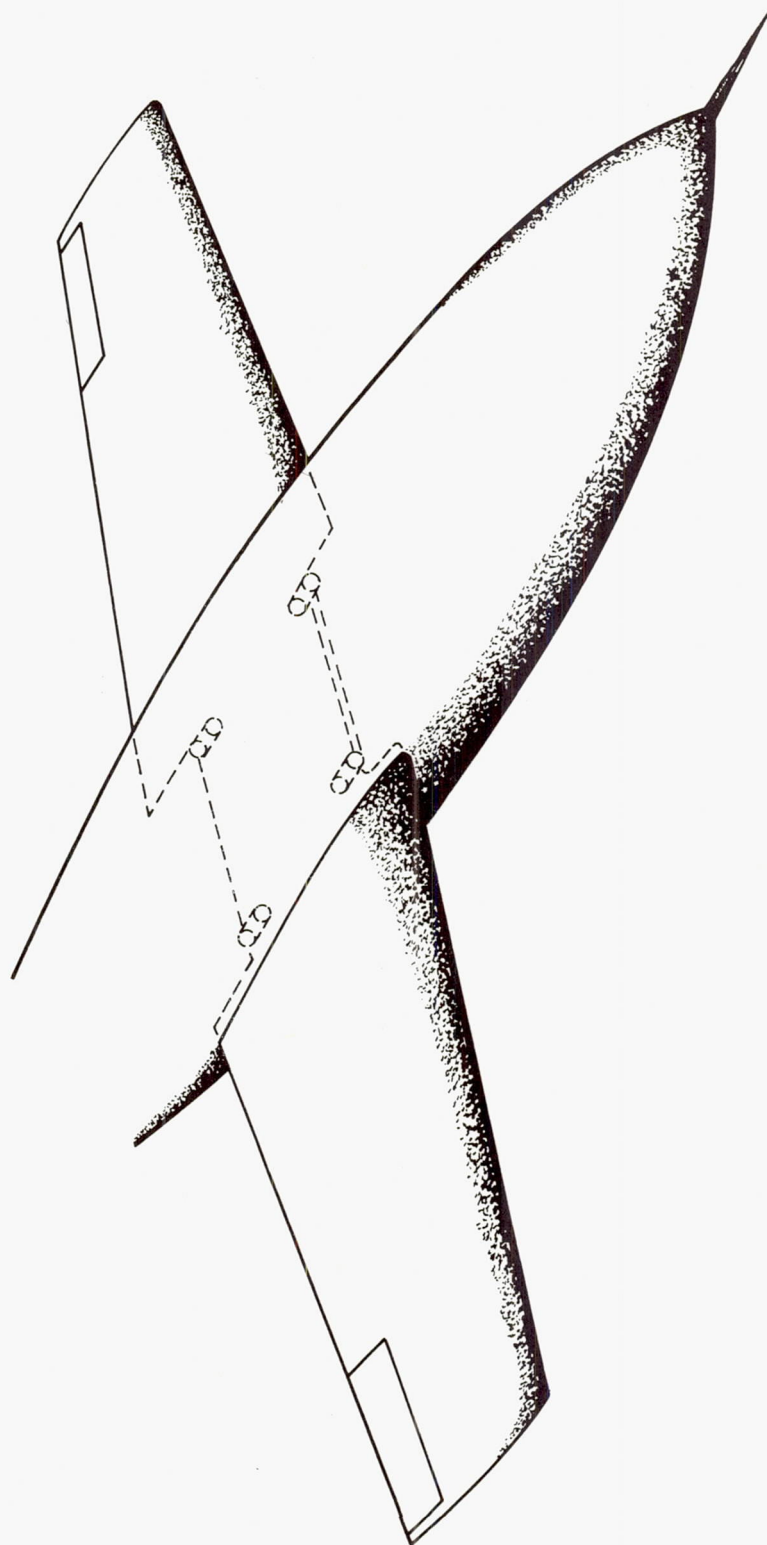
(b) Sketch showing four-point suspension of wing.

Figure 2.- Continued.
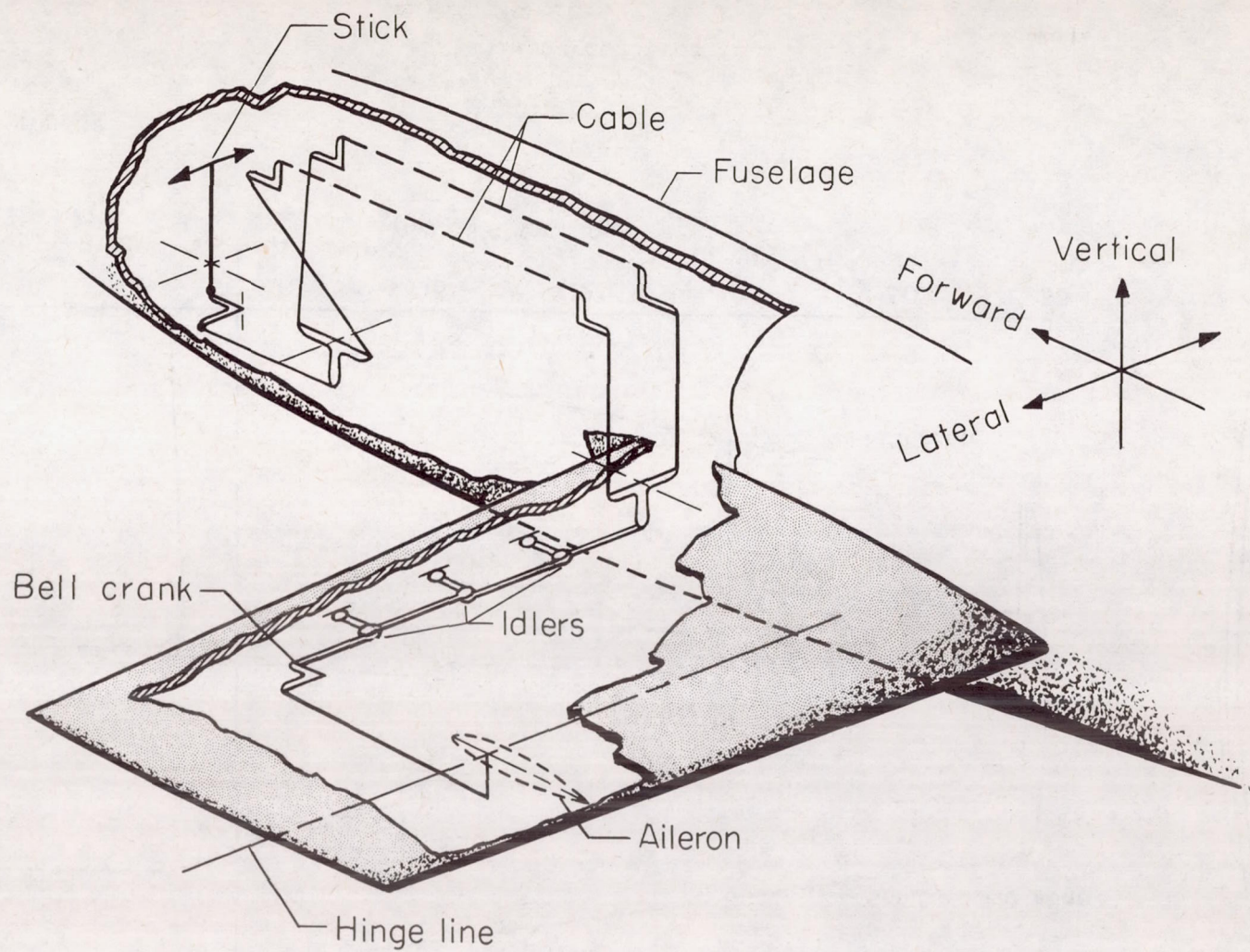
(c) Schematic sketch of aileron control system.

Figure 2.- Concluded.

Section A—A

Doubler

Solid leading edge

Solid tip

Aileron

A

A

O   5   10   15   20   25   30   35

Wing station, in.

℄ Fuselage
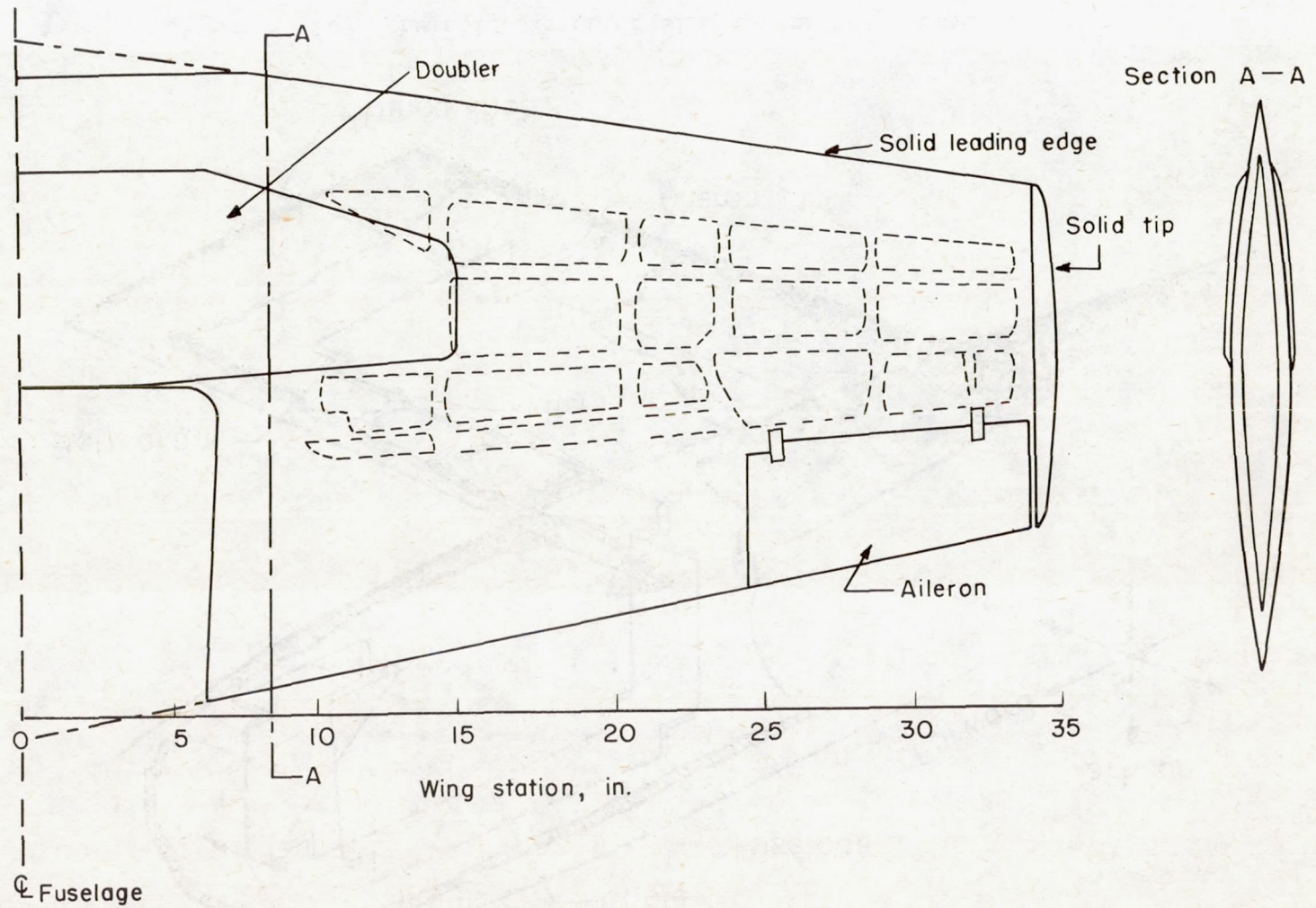
(a) Wing construction.

Figure 3.- Details of $\frac{1}{4}$-scale model of X-1E airplane.
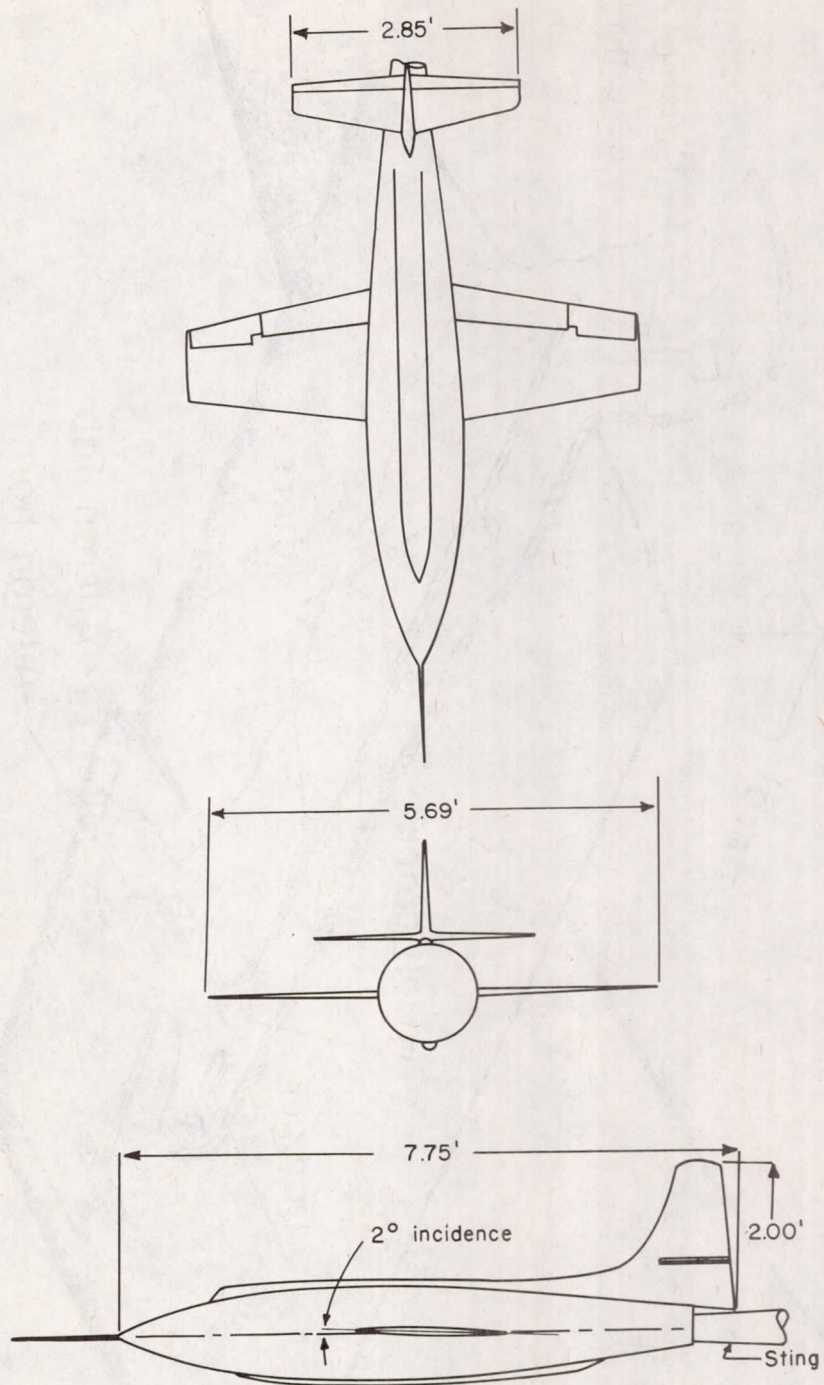
(b) Configuration of model.

Figure 3.- Continued.

Forward Vertical Lateral

Control column

Bell crank

Damper

Idlers

Aileron tab

Aileron horn
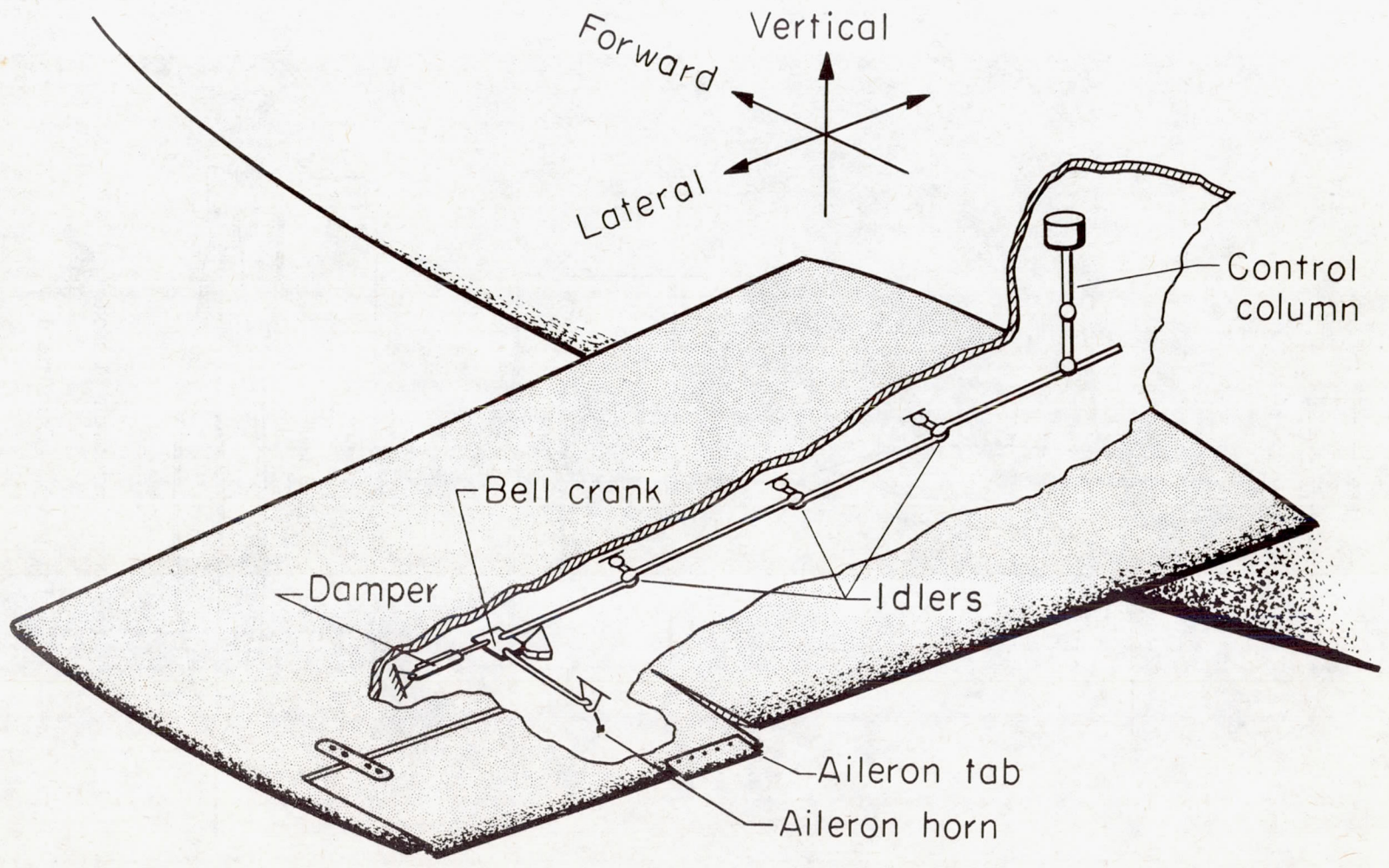
(c) Sketch of aileron control system.

Figure 3.- Concluded.
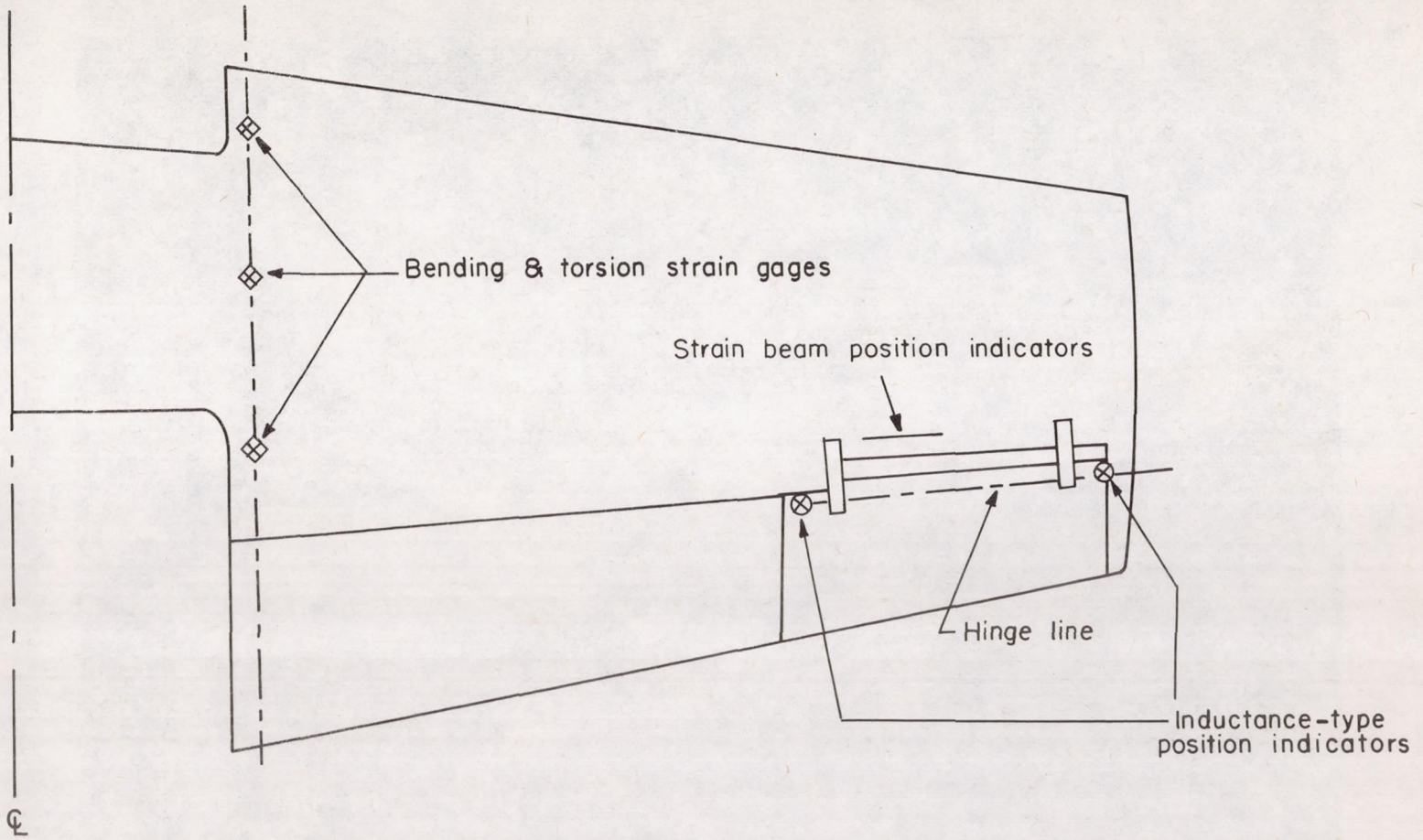
Figure 4.- Positions of instrumentation on $\frac{1}{4}$-scale model.
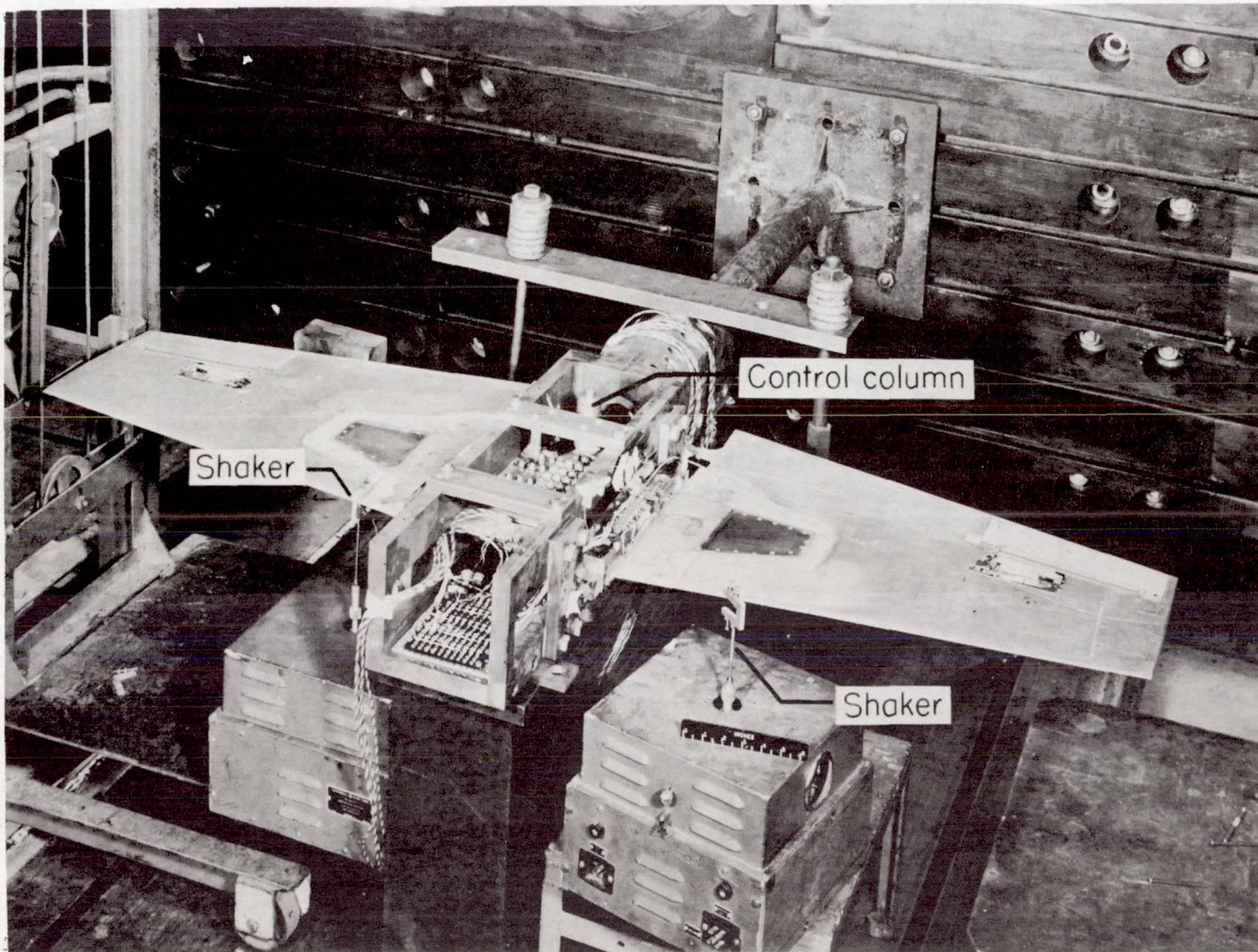
L-89734.1

Figure 5.- Model wing mounted for ground testing.
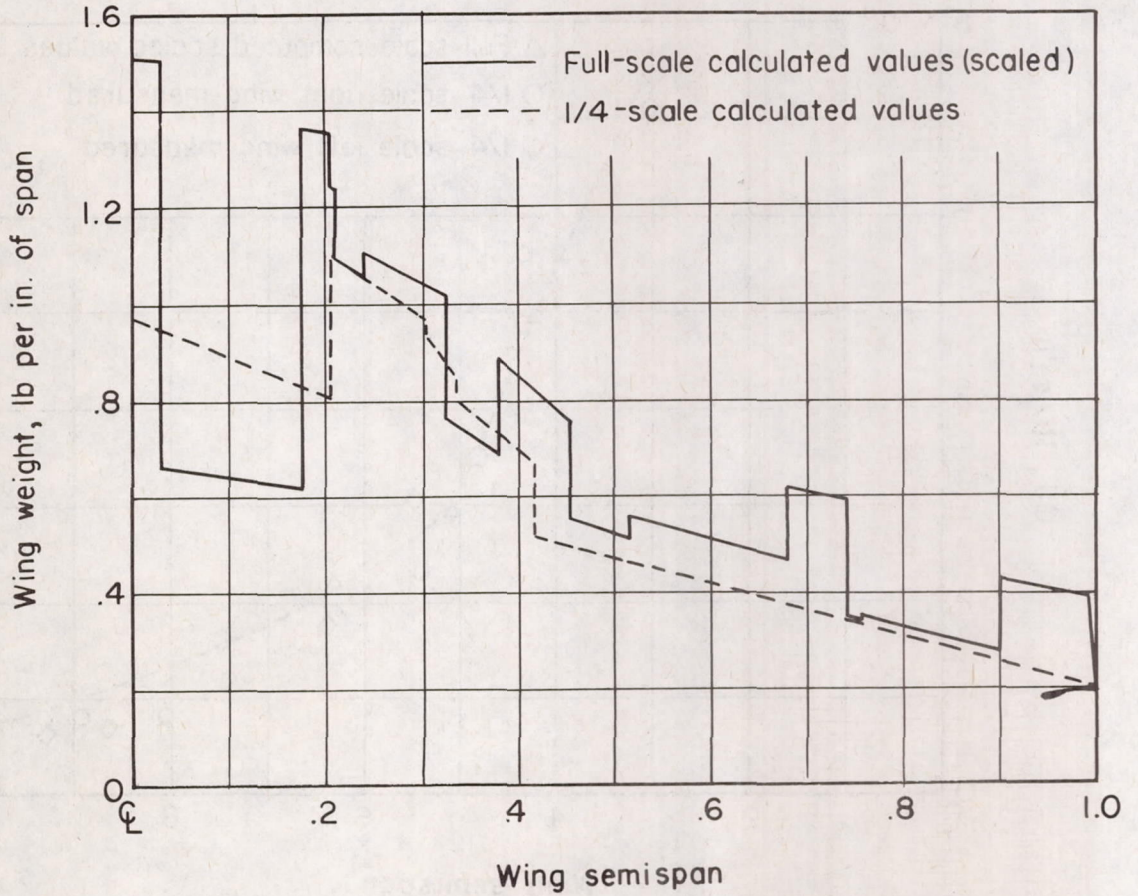
Figure 6.- Comparison of X-1E full-scale and $\frac{1}{4}$-scale spanwise weight distributions.
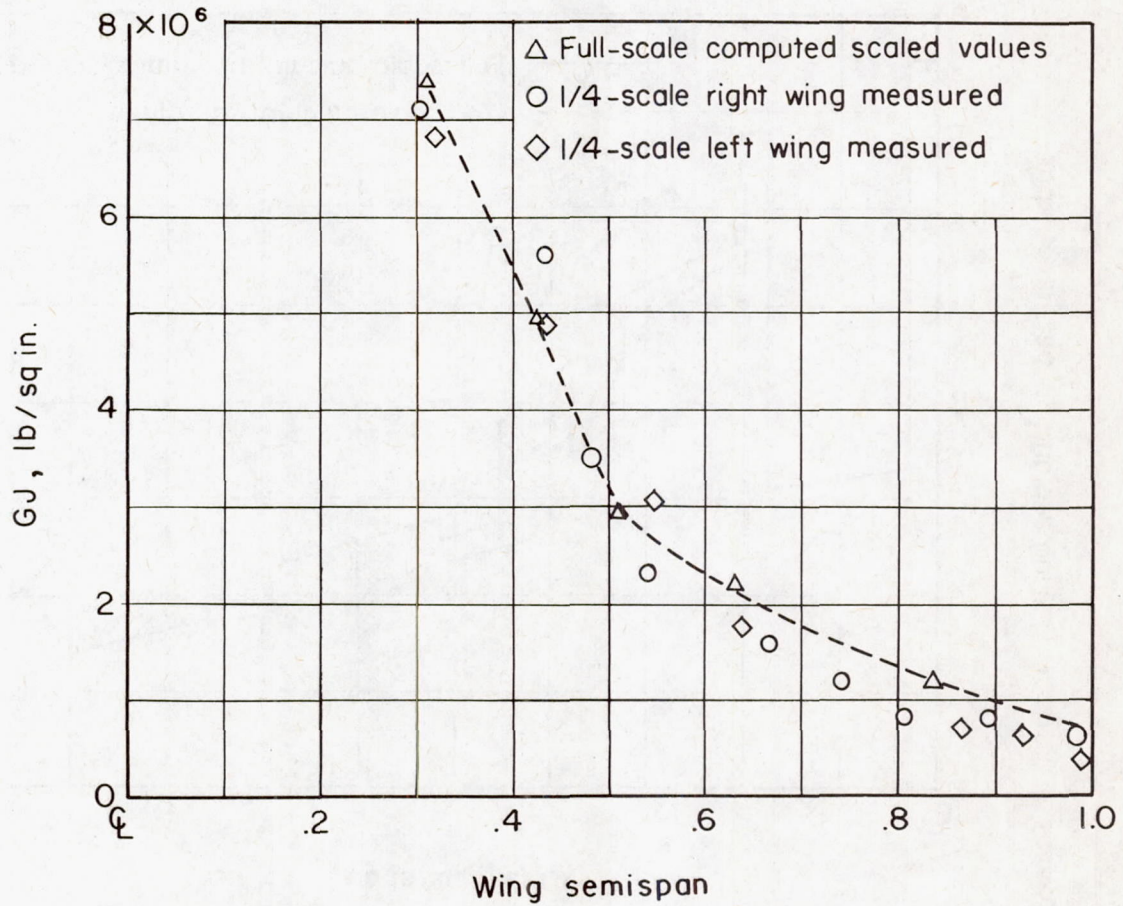
Figure 7.- Comparison of X-1E full-scale and $\frac{1}{4}$- scale torsional rigidity.
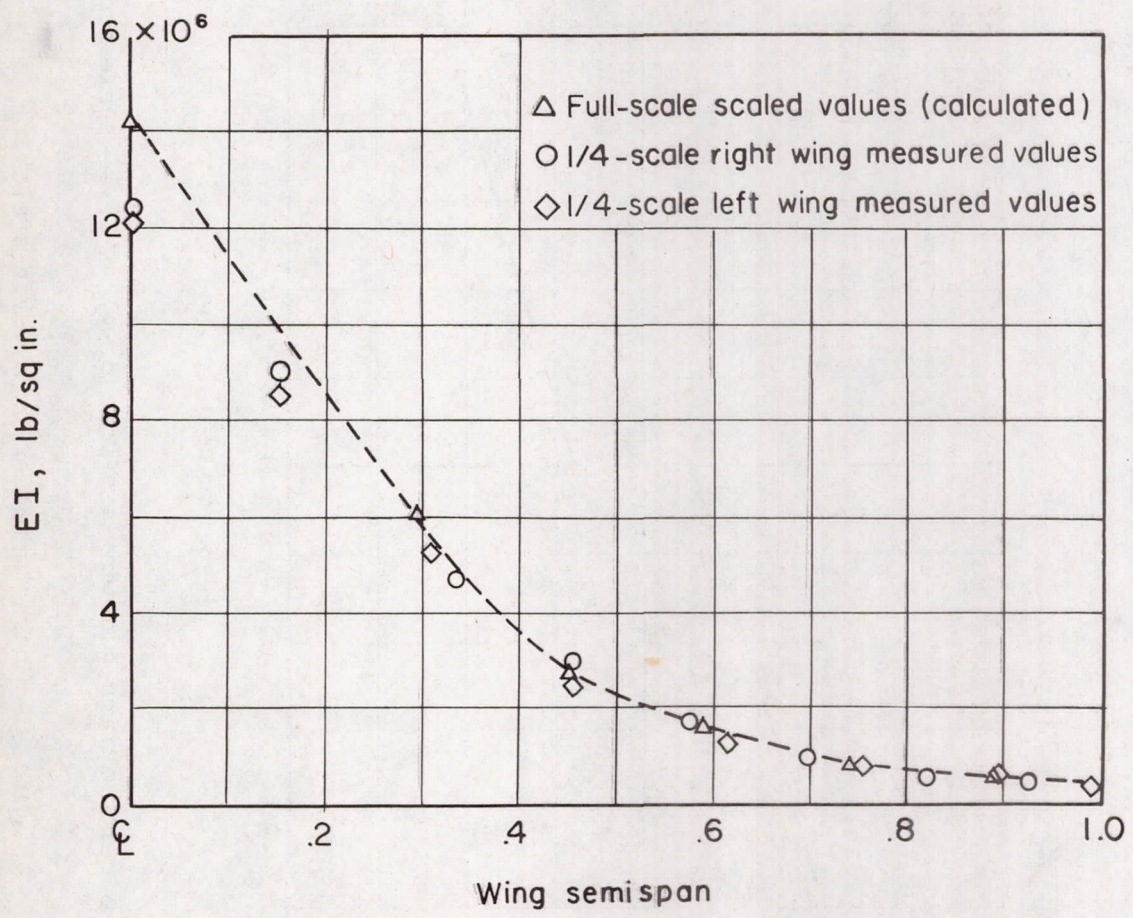
Figure 8.- Comparison of X-1E full-scale and $\frac{1}{4}$-scale bending rigidity.
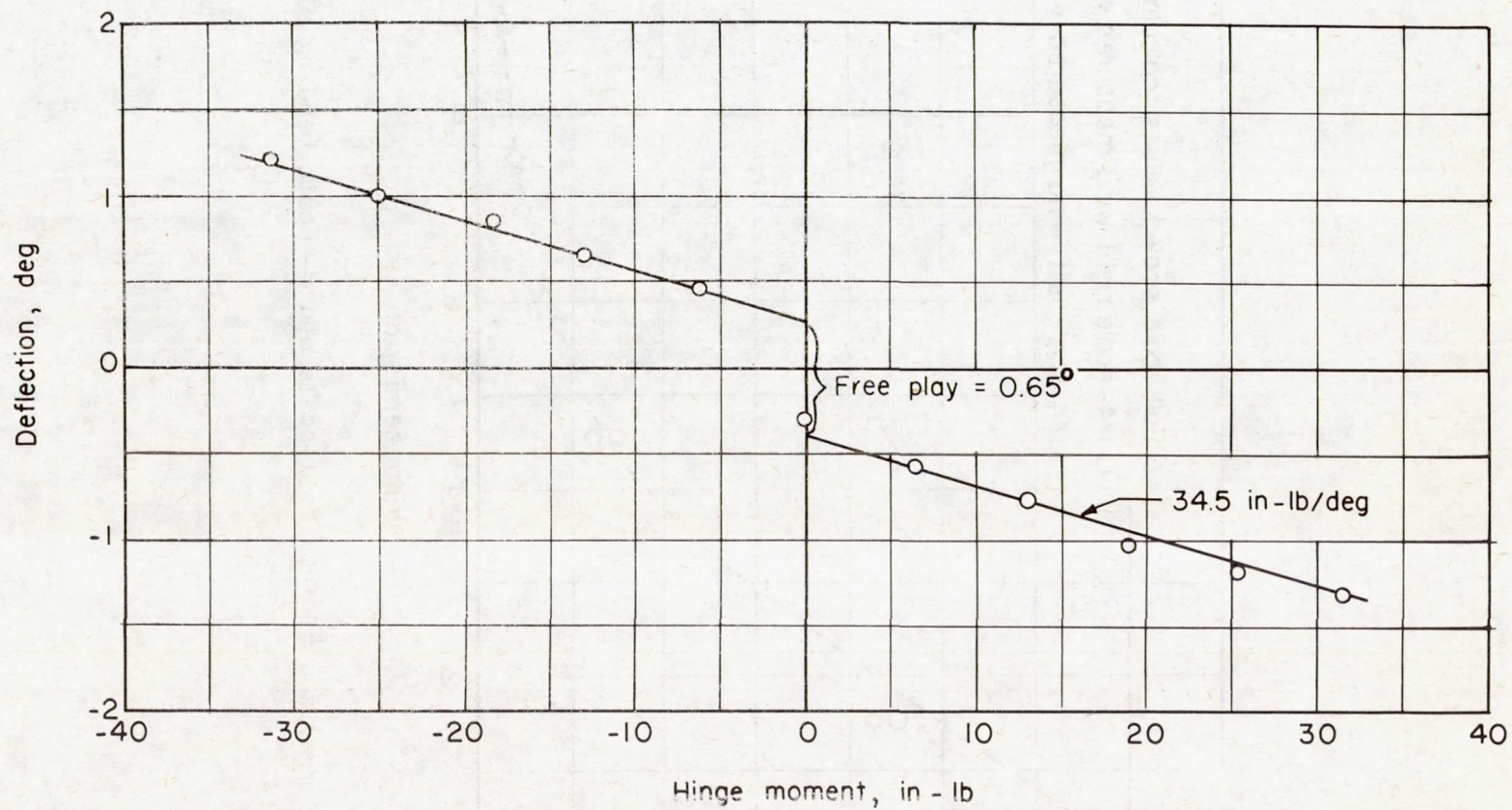
(a) Right aileron spring constant and free play. X-1E $\frac{1}{4}$ - scale model.

Figure 9.- Characteristics of aileron system.
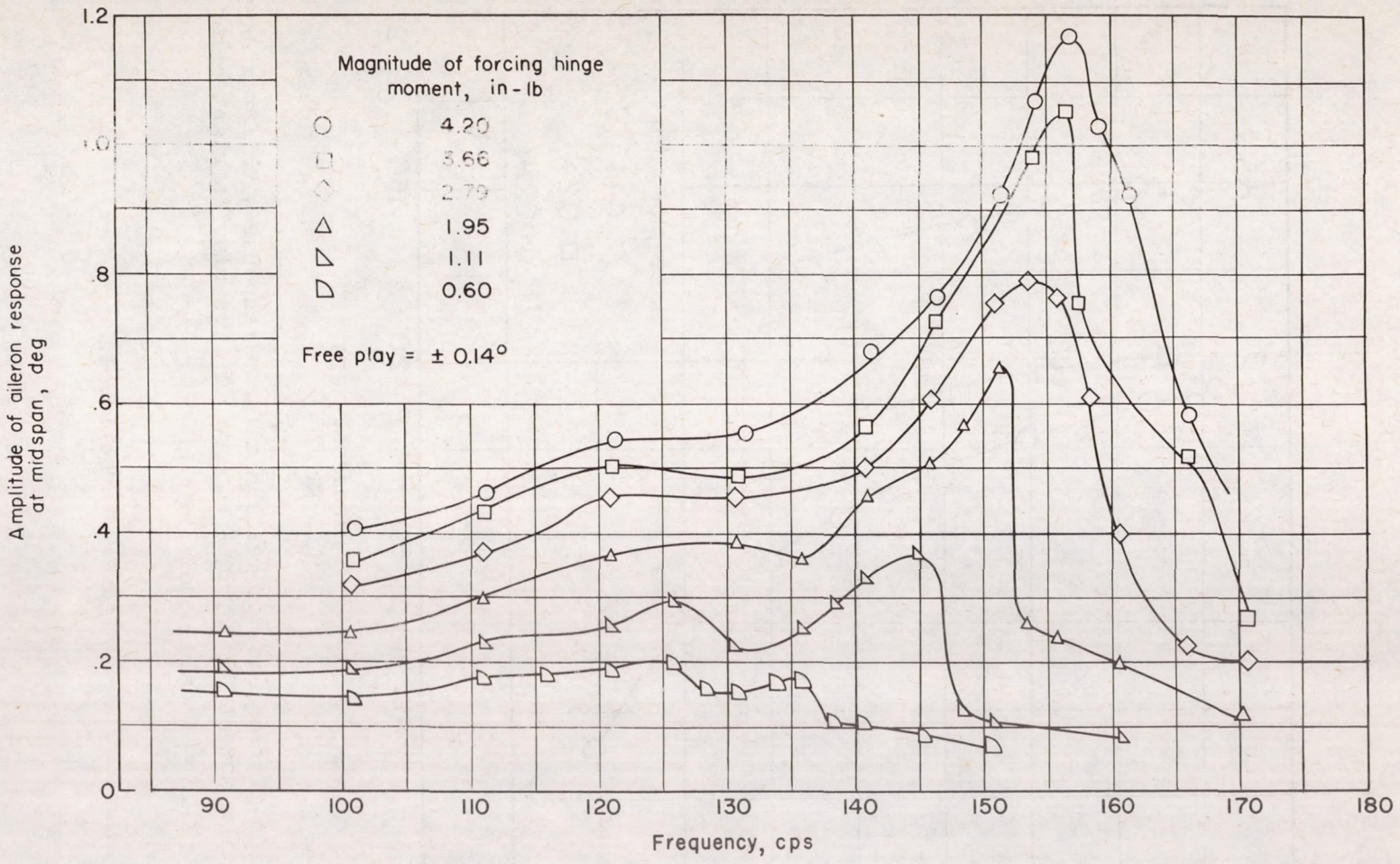
(b) Variation of amplitude and resonant frequency with excitation force. X-1E $\frac{1}{4}$- scale model aileron control column locked at fuselage center line.

Figure 9.- Continued.
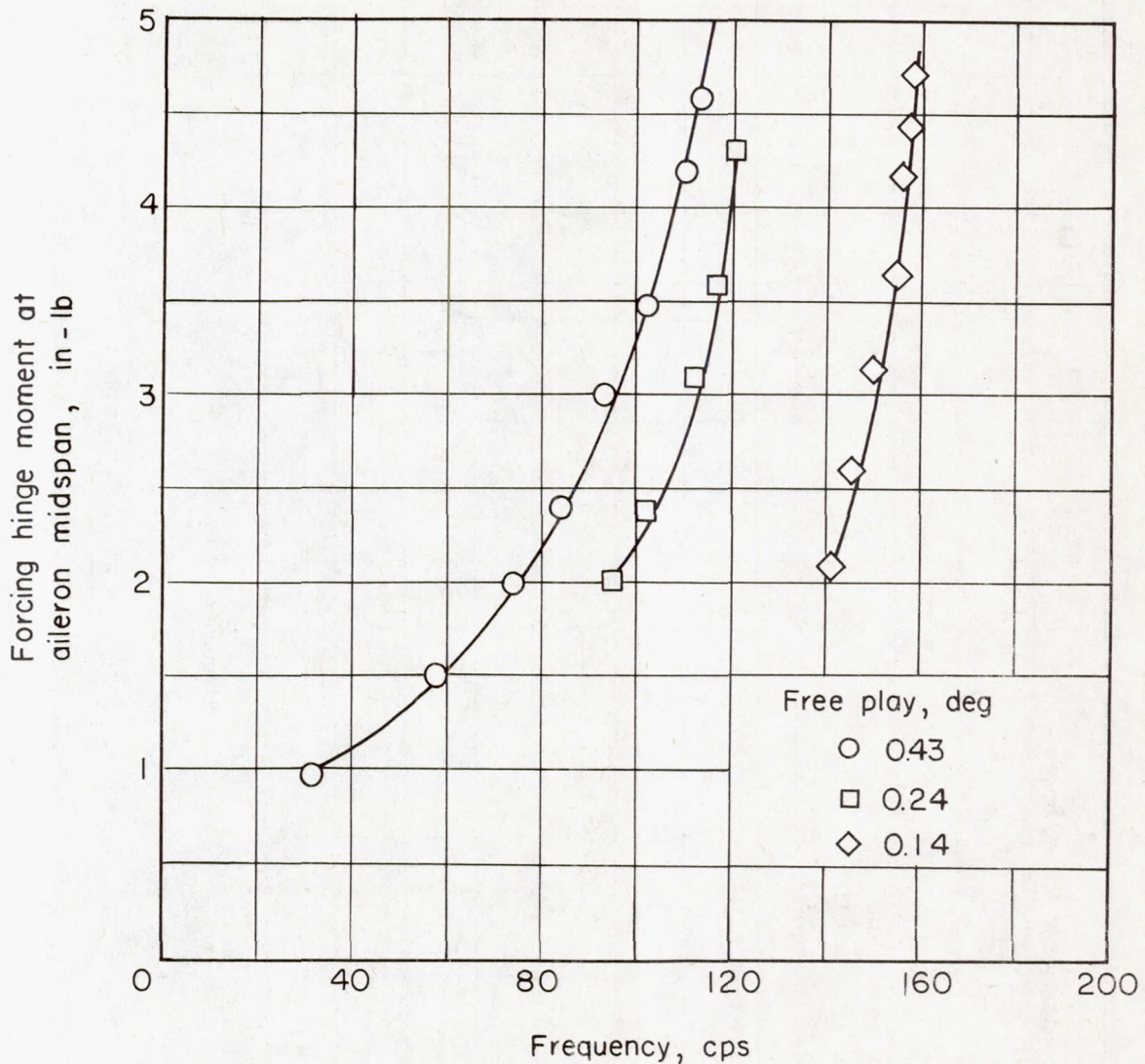
(c) Variation of frequency of maximum aileron response with air shaker oscillation moment for various amounts of free play in right aileron system. X-1E $\frac{1}{4}$ - scale model.

Figure 9.- Continued.
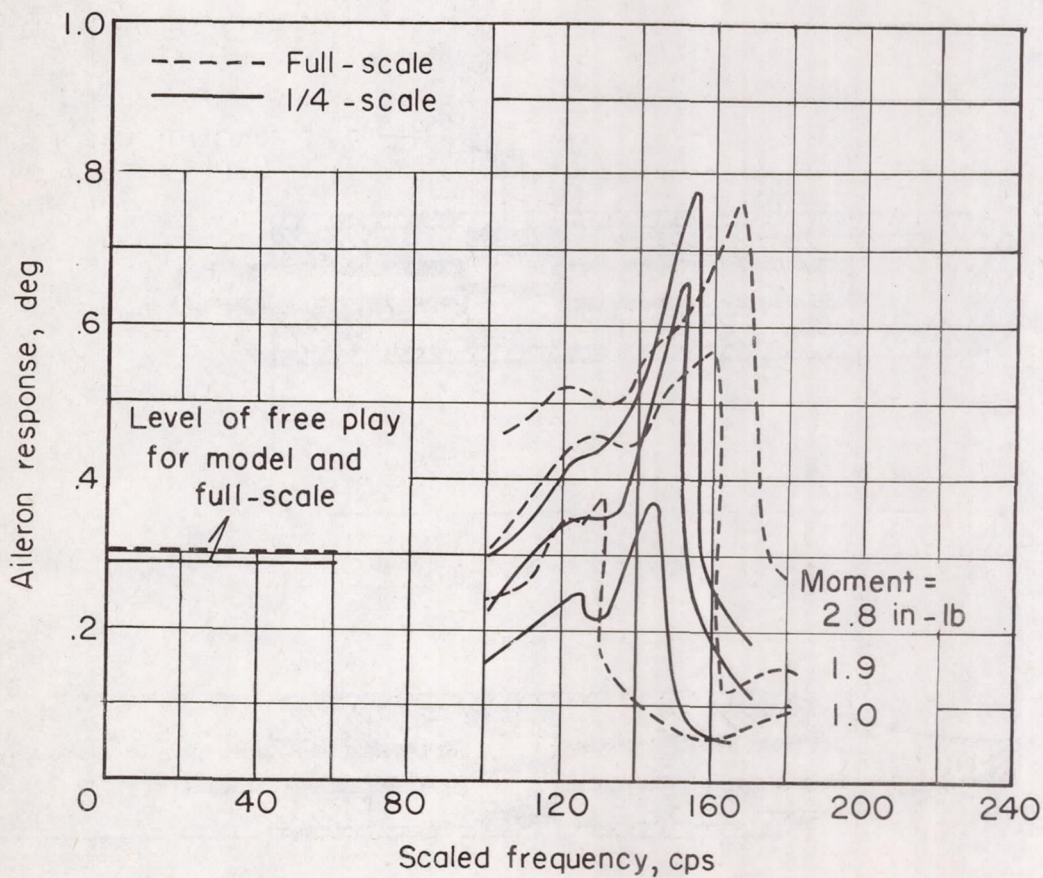
(d) Comparison of X-1E full-scale and $\frac{1}{4}$ - scale model aileron

frequency response.

Figure 9.- Concluded.

Inlet for hydraulic
fluid

3 "

3/8"
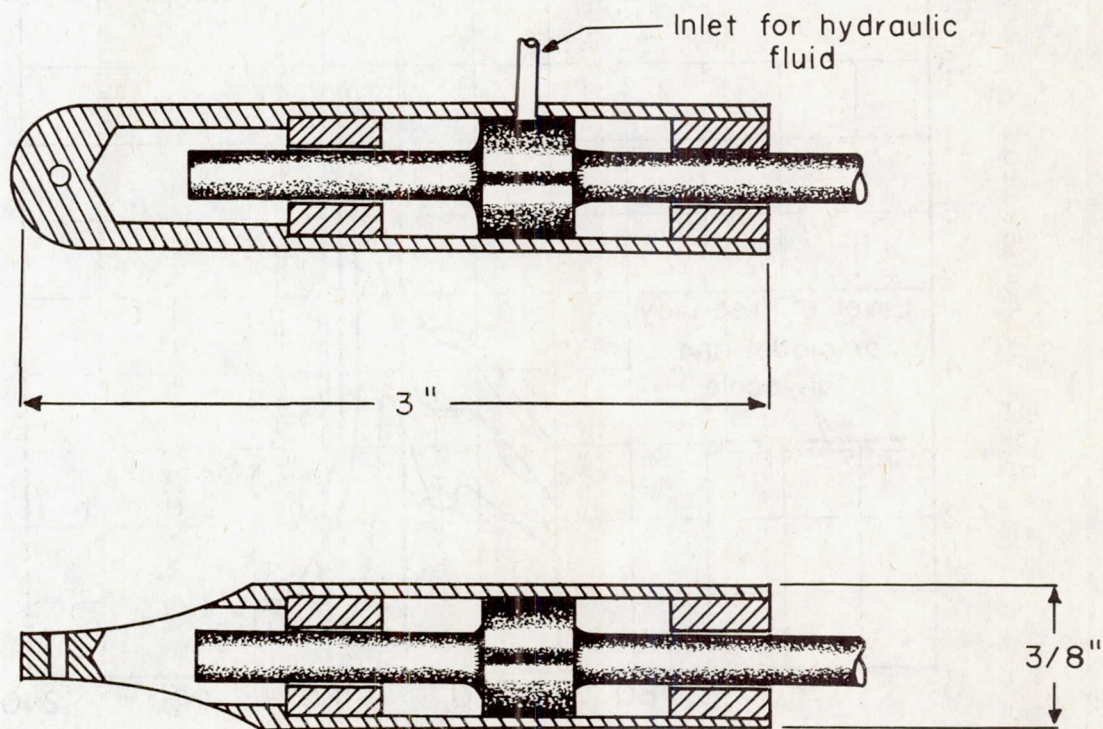
Figure 10.- Sketch of $\frac{1}{4}$-scale-model aileron damper.

...
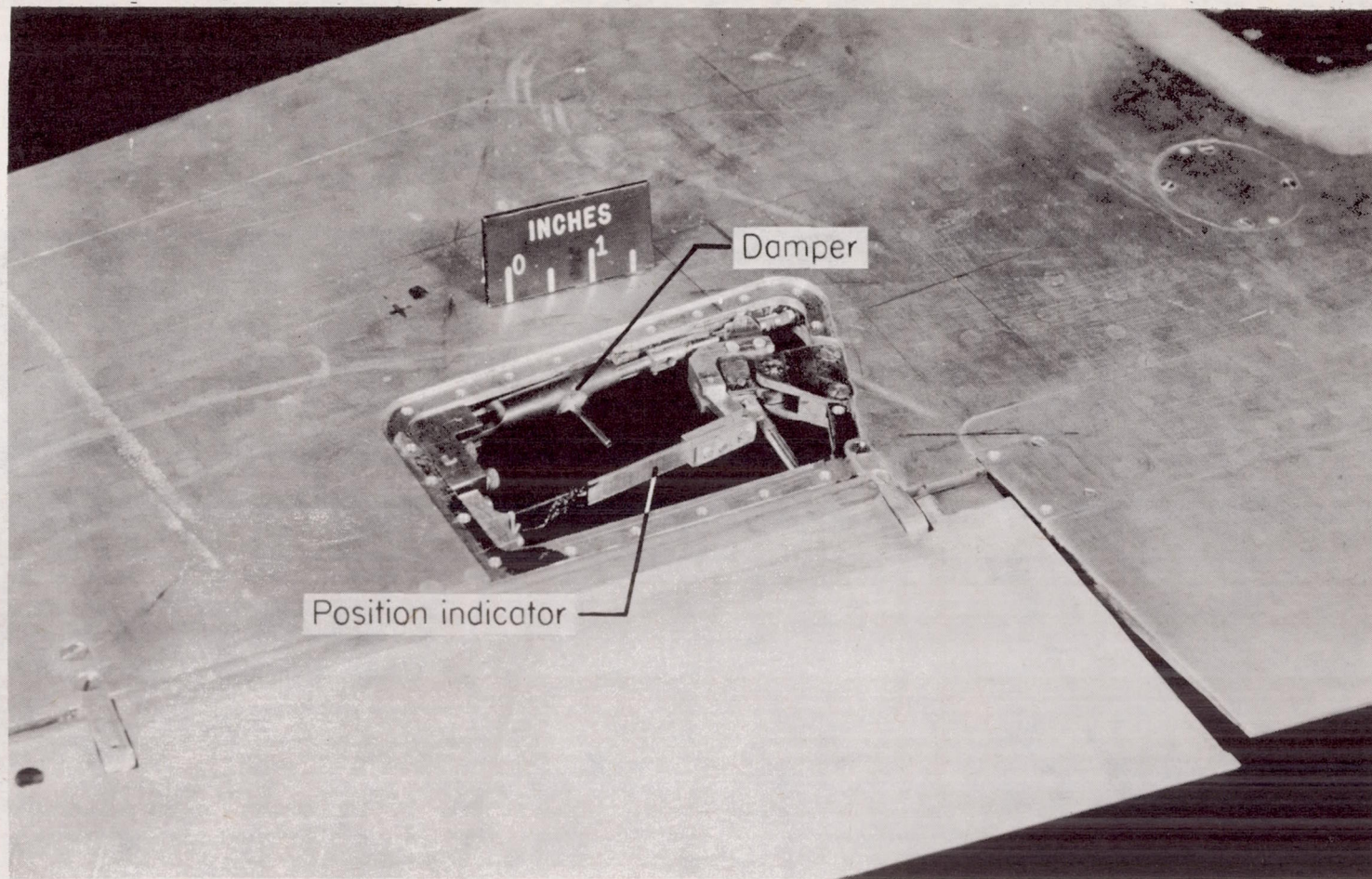
(a) Damper mounted inside wing (internal damper).   L-89730.1

Figure 11.- Damper installations for $\frac{1}{4}$- scale model.
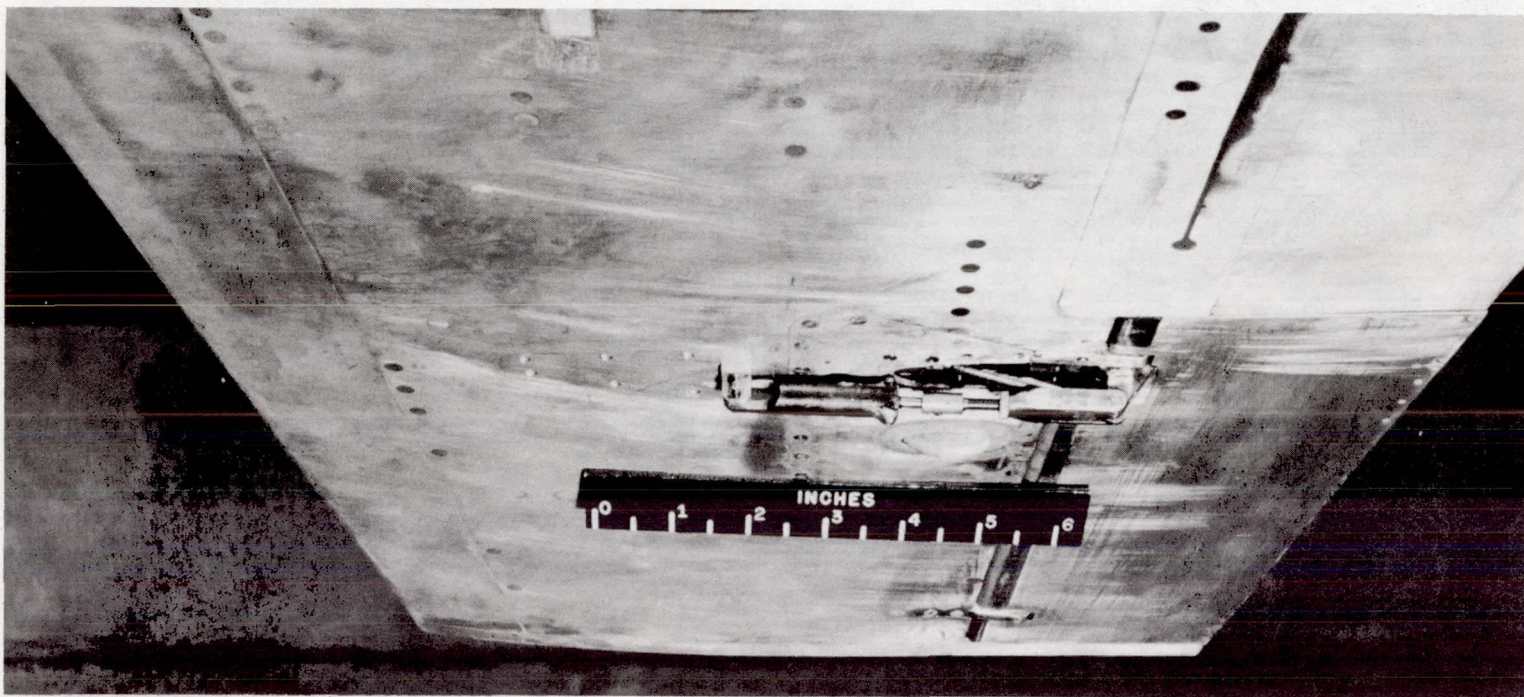
L-93043

(b) Damper mounted on under surface of wing (external damper) with fairing removed.
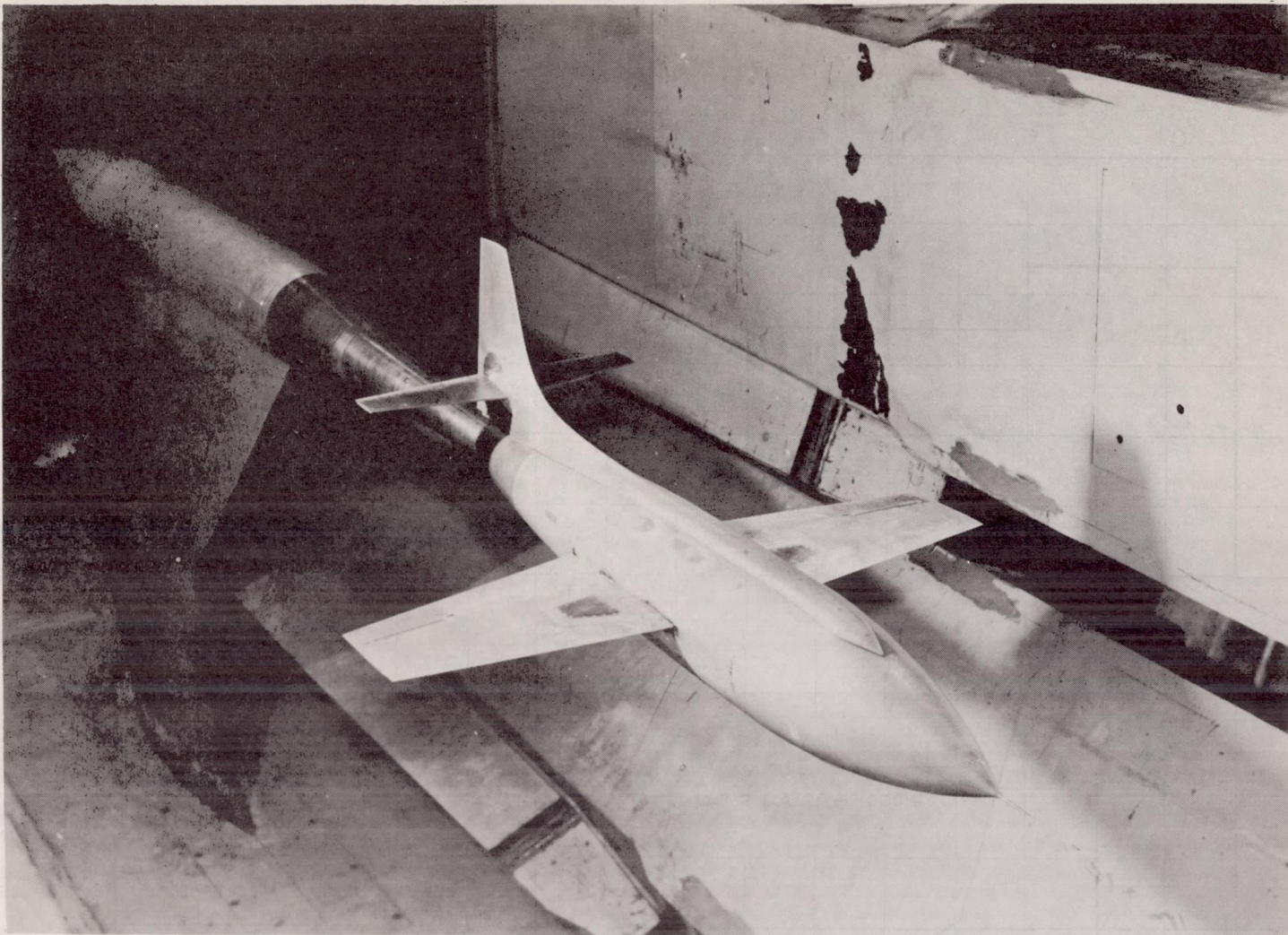
Figure 11.- Concluded.

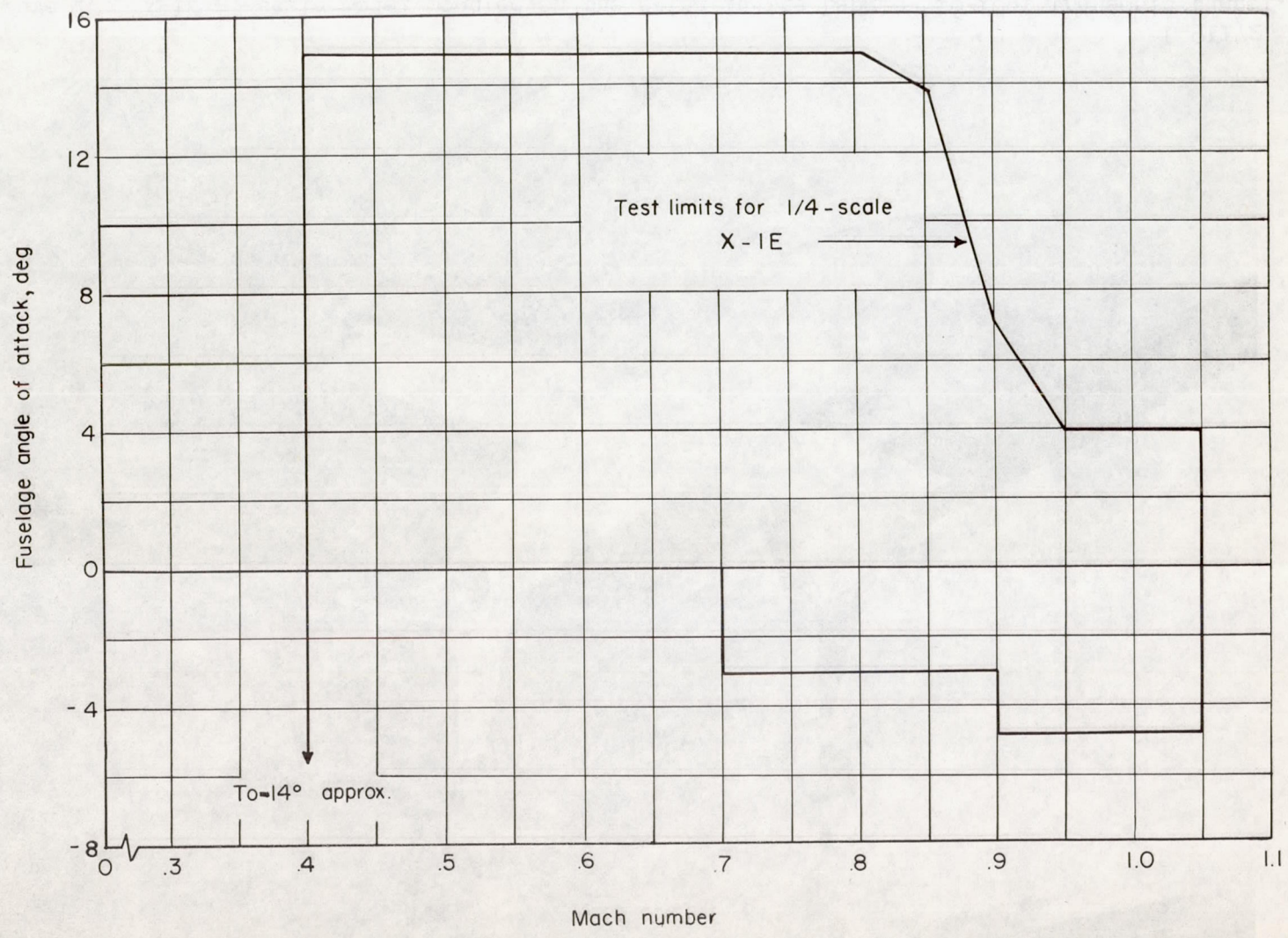Figure 12.- X-1E $\frac{1}{4}$-scale model mounted on the sting in the Langley 16-foot transonic tunnel.

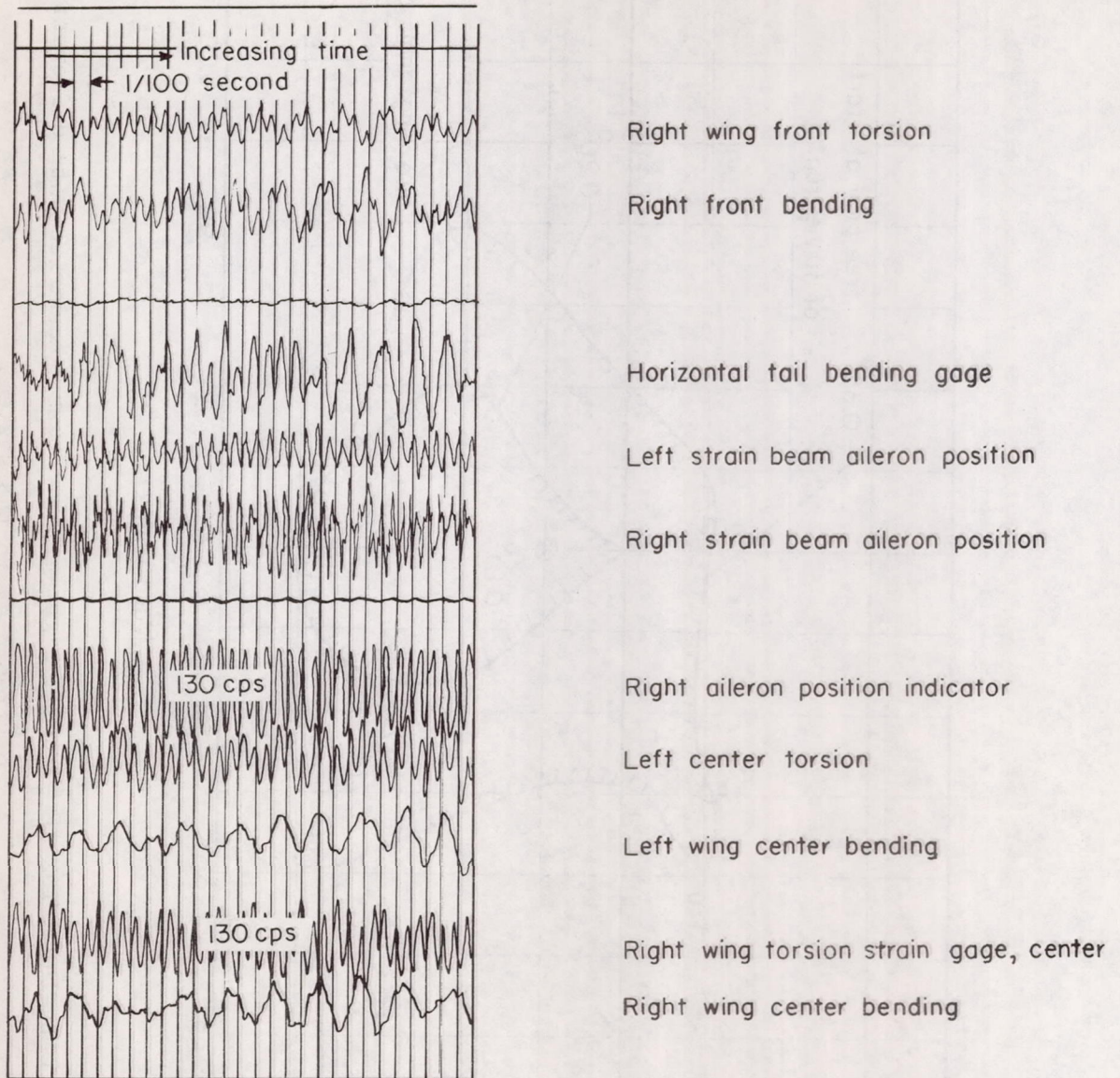Figure 13.- Test limits for $\frac{1}{4}$-scale X-1E model in Langley 16-foot transonic tunnel.

Figure 14.- Typical oscillograph record of aileron buzz. M = 0.93;
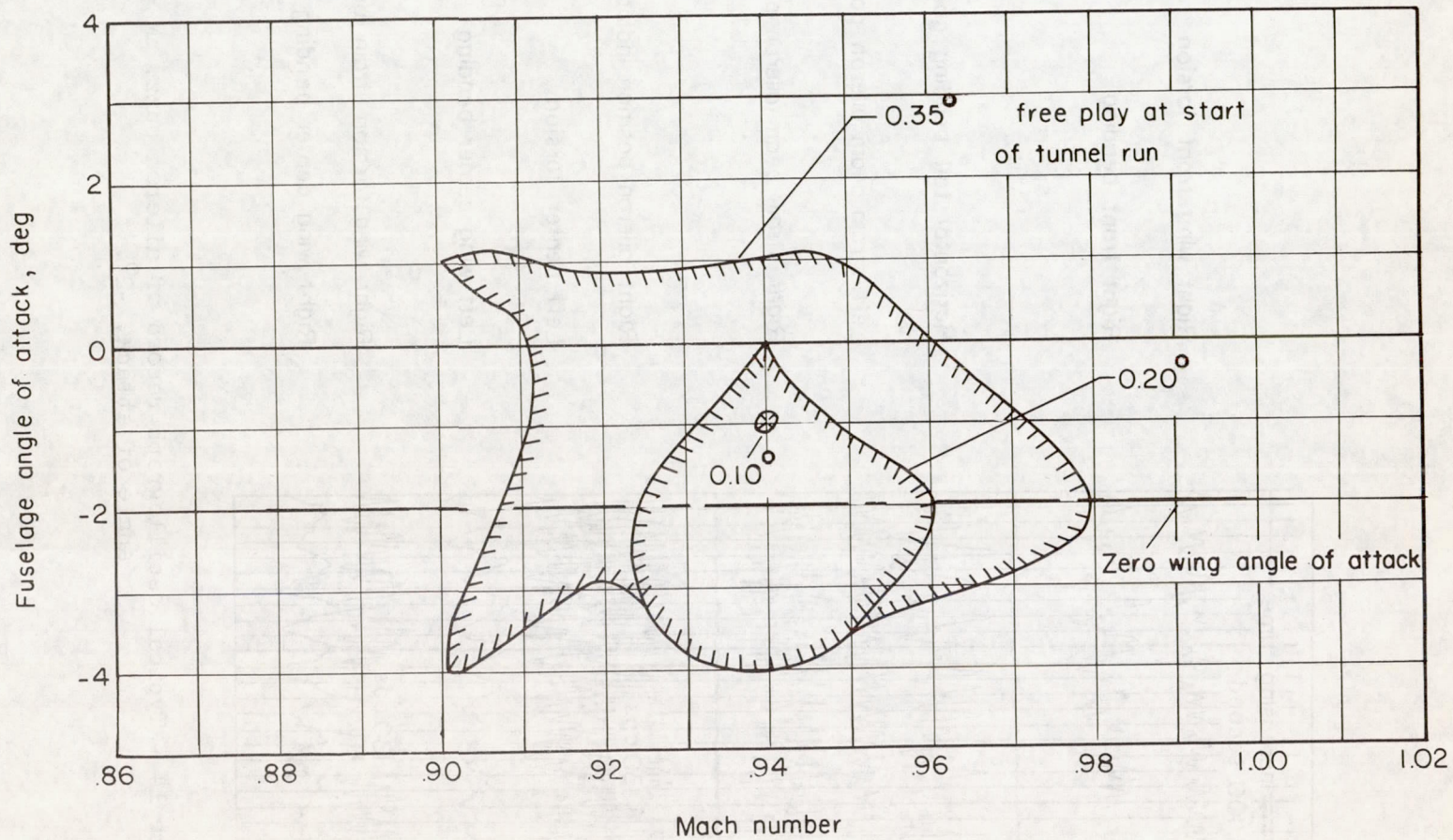angle of attack, -2°.

Figure 15.- Comparison of X-1E $\frac{1}{4}$ - scale right-aileron buzz boundaries with different degrees of free play in the system.